Analysis of tracer particle characteristics for micro PIV in wall-bounded gas flows

Sebastian BURGMANN*[1], Nadine VAN DER SCHOOT [1], Christof ASBACH[2],
Jens WARTMANN[1], Ralph LINDKEN[1]

[1]. *Zentrum für BrennstoffzellenTechnik ZBT GmbH, Carl-Benz-Straße 201, D-47057 Duisburg, Germany*
s.burgmann@zbt-duisburg.de, n.vanderschoot@zbt-duisburg.de, j.wartmann@zbt-duisburg.de, r.lindken@zbt-duisburg.de
[2]. *Institut für Energie– und Umwelttechnik e.V., IUTA, Bliersheimer Str. 60, D-47229 Duisburg, Germany*
asbach@iuta.de

ABSTRACT. – The investigation of the gas flow in a working fuel cell by means of optical measurement techniques like micro Particle-Image Velocimetry (µPIV) requires the generation of suitable tracer particles. In this work the analysis of tracer particle characteristics is described which serves as a means to identify suitable particles for wall-bounded gas flows. Several materials and different types of particle generators were examined to check for obtainable particle size distributions and particle concentrations. A simple experiment was designed to investigate the capability of the generated particles to adequately follow the flow. An optically transparent micro-channel with a 90° elbow was manufactured and the µPIV measurement technique is applied. Firstly, the gas-flow seeded with tracer particles is investigated within this 90° elbow micro-channel. Secondly, to check whether the measured flow structure in this previous case matches with the real flow, the same flow conditions are investigated using water as working fluid with solid tracer particles taking into account Reynolds number similarity. Thirdly, CFD-calculations using the same reference parameters as in the experimental investigations were performed to quantify the deviation of the particle traces from the real flow streamlines. The results show ethylene glycol to be a suitable tracer material since the obtained tracer particles are optically detectable without severe image post-processing and since this material can be easily transformed into an aerosol with suitable concentrations and particle size distributions. The application of the µPIV technique on such a gaseous particle laden flow provided promising results concerning the intended application of this technique to operating fuel cells.

Key-words : particle-image velocimetry, particle generation, particle traces, response time, fuel cell.

Analyse des caractéristiques de traceurs pour la micro PIV dans des écoulements gazeux confinés

RESUME. L'étude de l'écoulement gazeux dans une pile à combustible au moyen de techniques de mesure optique telles que la micro vélocimétrie par imagerie de particules (µPIV) nécessite la mise au point de particules traceuses appropriées. Nous décrivons ici l'analyse des caractéristiques de ces particules afin d'identifier les particules convenables pour des écoulements confinés. Plusieurs matériaux et différents types de générateurs de particules sont testés en analysant les distributions de taille et les concentrations de particules. Une expérience simple a été conçue pour étudier la capacité des particules générées à suivre correctement l'écoulement. Un microcanal transparent coudé à 90° a été fabriqué pour analyser l'écoulement par la technique de µPIV. Tout d'abord, on étudie l'écoulement de gaz ensemencé par les particules traceuses dans ce microcanal coudé. Ensuite, pour vérifier que la structure de l'écoulement déduite de cette mesure correspond à celle de l'écoulement réel, les mêmes conditions d'écoulement sont étudiées en utilisant comme fluide de travail de l'eau ensemencée par des particules solides, en conservant une similitude de Reynolds.

Enfin on réalise des simulations numériques avec les mêmes paramètres de référence que dans les études expérimentales, pour quantifier la déviation des particules traceuses par rapport aux lignes de courant de l'écoulement réel.

Les résultats montrent que l'éthylène glycol est un traceur convenable car les particules obtenues sont décelables optiquement sans nécessiter un traitement d'image élaboré, et car il peut facilement être transformé en aérosol avec des concentrations et des distributions de tailles adaptées.

L'application de la technique de µPIV à un écoulement gazeux ensemencé donne des résultats prometteurs quant à l'application de cette technique pour l'exploitation des piles à combustible.

Mots-clés : PIV, Vélocimétrie par imagerie de particule, génération de particules, trace de particule, temps de réponse, pile à combustible

---

* Corresponding author

1. INTRODUCTION

In the last decade micro-scale Particle Image Velocimetry (µPIV) established as a standard measurement technique to investigate velocity distributions in microscopic devices with characteristic length scales of 10^{-3}m to 10^{-7}m. The motion of the fluid, which usually is a transparent liquid, is made observable by adding small tracer particles. The region of interest is illuminated by a laser such that the particles can be optically detected by a camera. Recording two particle

images within a small time interval allows the reconstruction of the flow velocity distribution based on the particle image displacement. This technique is similar to the well known macro-PIV technique which is widely used in experimental fluid mechanics. Comprehensive reviews of this technique and its mathematical and optical basics are given by, e.g., [17]. However, μPIV involves different optical and geometrical constraints. In contrast to classical macro-PIV, which is based on the illumination of a single measurement plane using special light-sheet optics, μPIV employs a volume illumination, i.e., the complete depth of the, e.g., micro-channel, is illuminated. The measurement plane is defined by the depth-of-focus (or more precisely the depth of correlation [16]) of the microscope optics. Furthermore, fluorescent particles are used in μPIV applications to overcome the significant background noise due to the volume-illumination, i.e., the particles that are stimulated by the (green) laser light emit light of a different wavelength (usually red light). Applying optical filters the signal of the particles can be separated from the background noise. I.e., it is not the Mie-scattering of the illuminated particles that is detected in μPIV-configurations but the fluorescence of a dye added to the particles. This technique affords a different illumination setup than in macro-PIV applications : the laser beam and the fluorescent light emitted from the particles both pass through the lens of the microscope resulting in a complex optical set-up consisting of a dichroic mirror and an optical filter. The principle of μPIV is sketched in Fig. 1. Further details on the μPIV techniques, interesting examples, and practical advices can be found in [21] and [13].

Microfluidic devices usually operate with liquid fluids. However, in some cases gaseous flows in micro-channels become more and more of interest. Often the gaseous fluid can be substituted in the experiment by a liquid simply by applying Reynolds analogy. This ordinary way cannot be applied if other important effects are eliminated by this approach, e.g., electrochemical processes like in fuel cells. However, the fluid mechanical processes within fuel cells are not completely understood. One of the major topics of fluid mechanical research concerning fuel cells is the homogenous distribution of the reactants, e.g., oxygen and hydrogen in case of a proton-exchange membrane (PEM) fuel cell, within the cell. This aspect becomes highly complex due to electrochemical processes within the cell, e.g., changes of volume fluxes due to chemical reactions, or thermodynamic effects like the transition from gaseous to liquid water in the cell. Electrically conductive panels with micro-channels are
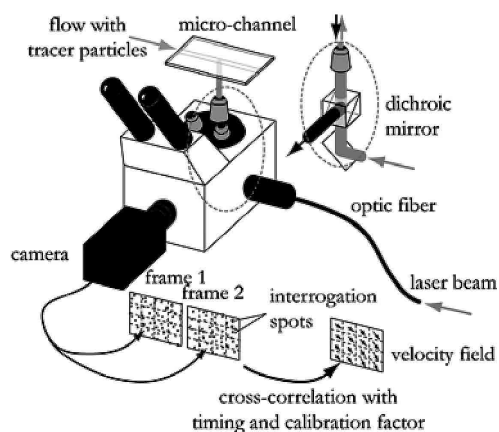
commonly used to distribute the reactant gases. The structure and arrangement of the micro-channels on these panels are part of ongoing research concerning the homogeneous distribution of the reactant gases and the corresponding pressure losses [11], [12], [23]. The fluid mechanical characteristics within the micro-channel structure of the plates is far from being completely understood. One promising way to get a deeper understanding is the application of optical measurement techniques like Laser-Doppler Velocimetry (LDV), PIV or μPIV. These measurement techniques are based on the detection of small particles. It is therefore inevitable to adequately seed the flow, i.e., the particles need to be detectable and need to follow the flow with high fidelity. Furthermore, the seeding particles may not change the electrochemical processes or have any other disturbing effect on the performance of the fuel cell. Several groups applied PIV measurement techniques to fuel cells or fuel cell-like configurations. In most of these investigations assumptions and simplifications have been made to make the specific measurement technique applicable. Most of the investigations are performed in scaled models such that the classical light-sheet technique could be applied [2, 3, 7, 10, 15, 25]. However, even in those cases the deviation of the particle traces needs to be addressed concerning gas-phase measurements, since the flow velocities are large and the branch-structure of fuel cells is complex and narrow. Some groups performed μPIV measurements. Concerning gas-phase flows problems occur concerning the generation and feeding of suitable particles to the micro-channels [5, 18]. Note the μPIV technique is directly applicable to a fuel cell-like arrangement without restrictions concerning electrochemistry if the reactant fluid is a liquid like in a direct methanol fuel cell (DMFC). μPIV measurements in such a fuel cell have been demonstrated, e.g., by [20]. To our knowledge there is only one experimental study on the flow in fuel cells using LDV. The method was shown to work in fuel cells but the results need to be regarded as preliminary [9].

In conclusion, the flow inside an operating PEM fuel cell has not been thoroughly analyzed using tracer particle based optical laser techniques, yet. The transparency of the channel-structures does not seem to be a critical issue. The key mechanism for the application of these measurement technique is the generation of suitable particles and the appropriate feeding of the fuel cell channels with particles. This study deals with the identification of suitable materials and particle generators, the characterization of the particle properties and the application of these particles in μPIV measurements in operating fuel cells.

The paper is organized as follows : in the following section the physics of tracer particles in μPIV applications will be explained. The second paragraph deals with the experimental results concerning the particle characteristics of ethylene-glycol based aerosols and gas-phase μPIV measurements in micro-channels. The paper closes with a final discussion and conclusion.

Figure 1 : *Sketch of a typical μPIV set-up using an epi-fluorescent inverted microscope.*

2. PARTICLE CHARACTERISTICS FOR μPIV-APPLICATIONS

2.1. The Ability of Particles to Follow the Flow

Usually microfluidic devices operate with liquid fluids which is advantageous for the application of μPIV. In this case it is quite comfortable to seed the flow with fluorescent

tracers since these particles can be easily pre-mixed into the working fluid. Furthermore, the commonly used PSL or MF particles possess a density which is similar to the density of the working fluid (ρ_{PSL} = 1.05 g/cm^3 and ρ_{MF} = 1.51 g/cm^3). Hence, deviations of the particle trace from the streamlines due to inertia effects are very small or even negligible. For gas flows the mapping of the flow structure using particle traces is more critical, since the particle density is usually several orders of magnitude higher than the density of the gas, e.g., DEHS (Di-Ethyl-Hexyl-Sebacat) particles with ρ_{DEHS} = 0.912 g/cm^3 in air (ρ_{air} = 0.001225 g/cm^3).

The relation of the density difference and the deviation of a particle from the streamline will be explained in the following. A small spherical particle with diameter d_p, density ρ_p and a relative mass $m_{p,rel}$ is moving in the surrounding fluid with a relative velocity of $u = U - u_p$ and is accelerated with du_p /dt :

$$F_D = m_{p,rel}\frac{du_p}{dt} \Leftrightarrow \frac{3\pi\eta u d_p}{C_c} = (\rho_p - \rho)\frac{\pi}{6}d_p^3\frac{du_p}{dt}. \quad (1)$$

where η represents the viscosity of the fluid, and ρ denotes the density of the fluid [1]. The formula on the left is valid for $Re_p < 1$ and is called Stokes law [2]. The parameter C_C accounts for the slip-effect of the particles in accelerated flows [6]. The corresponding dimensionless parameter that can be used as an indicator whether the particle traces are identical to the streamlines or not is the Stokes number St. For $St \to 0$ the particles follow the flow. The Stokes number can be expressed as (compare, e.g., [25]) :

$$St = \frac{\rho_p d_p^2 U\, C_c}{18\eta L}, \quad (2)$$

where ρ_p denotes the density of the particle, U is the flow velocity, and L is the characteristic length scale of the flow. This simple formulation applies for heavy particles in gas flows. Note, in this case for small particles, i.e., $d_p \leq 1$ µm a slip correction has to be taken into account, e.g., $C_C = 1.15$ for 1 µm particles [6] [3]. E. g., the Stokes number for 1 µm MF DEHS particles at 1 m/s in a 1 mm^2 micro-channel would be $St \approx 3\times10^{-3}$. I.e., the particle traces can be assumed to be identical with the stream lines.

The Stokes number only gives a hint on the ability of a specific particle depending on material and size to track the flow. A more practical way is the calculation of the response or relaxation time τ of a particle to a sudden change of the flow velocity and the determination of the corresponding drift length s_p. This relaxation time is mainly governed by inertia effects and can be derived from eq. 1. Rearranging this equation leads to :

$$U - u_p = \frac{(\rho_p - \rho)d_p^2 C_c}{18\eta}\frac{du_p}{dt} \; \blacktriangleright \; u_p = U\left(1 - e^{-t/\tau}\right),$$

$$\text{with } \tau = \frac{(\rho_p - \rho)d_p^2 C_c}{18\eta} \quad (3)$$

In contrast to the Stokes number the relaxation time can be used as a direct measure of the deviation of the particle traces from the flow direction. Imagine a particle starting with $u_p = U$ that is supposed to map a streamline that is equivalent to a quarter-circle curved path with radius r. Due to inertia this particle will deviate from this path. The centrifugal velocity can be expressed as $U_C = \tau\, U^2/r$. The time to travel this quarter-circle is $t = 2\pi\, r/(4U)$. Hence, the deviation of the particle from the streamline can be calculated as :

$$s_{p,\tau} = U_C\, t = \frac{\pi}{2}\tau\, U. \quad (4)$$

Concerning the micro-channel structure of the bipolar plates in fuel cells this is a quite important aspect that needs to be addressed if particle-based optical measurement techniques are to be used. Typical Reynolds numbers are in the range of $Re_a = 10$ at the anode side and $Re_c = 250$ at the cathode side. Since the density of a hydrogen flow at the anode side is very low, a particle based technique like PIV will not properly work due to the particle deviation. However, the Reynolds number of the anode-side flow is low and the flow is mainly influenced by friction. In other words, three-dimensional flow structures or separation zones are not likely to occur, which may afford a deeper investigation by an experimental method. Furthermore, depletion layers do not occur at the anode side, since pure hydrogen is fed to the micro-channels. At the cathode side the corresponding mean velocities are in the range $U_C = 3.5$ m/s. Assuming an acceptable deviation of about 1 % of the micro-channel width for a 90°-elbow, i.e., $s_{p,\tau} = 10$ µm for a 1 mm channel at a mean velocity of 3.5 m/s this leads to a corresponding relaxation time of $\tau = 0.9$ µs. I.e., the maximum size of ethylene-glycol particles would be $d_p \approx 0.5$ µm. Note, an only slightly larger ethylene-glycol particle of a diameter of, e.g. 1 µm, would lead to a deviation of $s_{p,\tau} = 45$ µm, i.e., 4.5 % of the channel width. The simple calculation given above indicates that particles smaller than 1µm are more suitable for a reliable flow tracking at the given Reynolds number regime. Note, Brownian motion, that affects particles in the range of several hundred nanometer and below, does not severely alter the flow in the present cases, especially taking into account the statistical error of the PIV post-processing. This aspect has been thoroughly discussed in [14] and [19]. Furthermore, the error by Brownian motion can be eliminated if ensemble or correlation averaging methods are applied in the PIV evaluation [21].

2.2. The Detectability of Particles in the Flow

Besides a high flow tracing ability particles need to be optically detectable. As mentioned before, in µPIV applications the fluorescent light of the particles is detected by the camera. Typically, liquid particle material is mixed with a fluorescent pigment and solid particles are coated with a fluorescent dye. Several different fluorescent dyes are available for µPIV applications, e.g., Rhodamine-B (excitation wavelength λ_{ex} = 560 nm, emission wavelength λ_{em} = 584 nm), Nile Blue A (λ_{ex} = 636 nm, λ_{em} = 680 nm) or Ethidium Bromide (λ_{ex} = 505 nm, λ_{em} = 602 nm). Since in most µPIV applications green lasers are used, e.g., frequency doubled Nd :YAG or Nd :YLF lasers with λ_{Nd-YAG} = 532 nm and λ_{Nd-YLF} = 527 nm, respectively, Rhodamine-B is a good choice, since the quantum efficiency of the fluorescence is relatively high, especially when dissolved in ethylene-glycol compared to a solution in water [1]. Rhodamine-B in crystalline form

---

1. Symbols without a subscript denote parameters of the fluid whereas the subscript p indicates characteristics of the particles.

2. The particle-Reynolds number is defined as : $Re_p = \rho d_p u/\eta$

3. Note, for particles with a density of the same order as the density of the fluid slip-effects are negligible, i.e., $C_C = 1$ applies for typical microfluidic applications in liquids.

can be easily dissolved in various liquids that can be used to generate an aerosol for PIV-measurements, e.g., water or ethylene-glycol. To dissolve Rhodamine-B in the oil DEHS or olive-oil usually a solvent like isopropanol is necessary. Note, the fluorescence of the fluid depends on the concentration of dissolved Rhodamine-B. However, as has been demonstrated for ethanol there is a critical concentration of Rhodamine-B, that determines the maximum intensity of fluorescence [22]. Several tests have been performed at our laboratory using different seeders and different liquids with Rhodamine-B and Rhodamine-B coated PSL particles concerning the detectability of fluorescent particles in a µPIV set-up. E.g., using a µPIV set-up in an 1mm micro-channel and an effective magnification of $M = 3.15$ and a 12bit PCO Sensicam QE CCD camera the ethylene-glycol particles with a concentration of 0.2 % Rhodamine-B induced a brightness of 950 counts, i.e., 23 % of the full-well capacity. The signal-to-noise ratio was 170 and the particle image was 4-16 pixels. In contrast, the 0.52 µm PSL particles (polymer microspheres, red fluorescing, 0.1 % solids) possessed a brightness of 150 counts, i.e., 4 % of the full-well capacity and a signal-to-noise ratio of 30. The average size of the particle image was 1-2 pixels which is to small for the application of PIV evaluation algorithms since the so-called peak-locking effect is likely to occur [17]. Further information concerning the detectability of Rhodamine-B admixed liquids can be found in [19].

2.3. The Generation of Tracer Particles

As depicted in the previous subsection coated PSL particles proved to be inadequate for µPIV applications in gas flows since these particles are hard to detect. Hence, liquid particles seemed to be a better choice especially since this special µPIV-technique is supposed to be applied to working fuel cells, i.e., solid particles would clog the porous layer of the MEA. Liquid droplets usually are formed by aerosol generators. There are several ways to generate small-scale liquid particles. E.g., in some apparatus a gas is injected into the liquid such that liquid is drawn into a high-speed gas-jet. Bubbles are formed that eventually burst. Small liquid droplets are released that are formed by the disrupting film or were embedded inside the bubble. A typical kind of such an atomizer is the Laskin nozzle aerosol generator. Another way to generated particles is condensation. In such a seeder small salt nuclei are generated that lead to a spontaneous droplet generation when they are injected into a highly saturated vapour steam. The particle concentration of such seeders like the Sinclair-LaMer generators is lower than that of atomizers. However, the droplets are monodisperse due to the fabrication process. Further details on the generation of particles can be found in [24].

Ethylene-glycol is a suitable particle material for µPIV applications since it can be easily nebulized into an aerosol. Furthermore, the viscosity and therefore the size of the particles can be easily changed by adjusting the temperature or by changing the amount of water in a water-ethylene glycol mixture. A similar manipulation cannot be done without great efforts, e.g., for DEHS. Using liquid droplets as tracer particles several aspects need to be addressed. E.g., the vapor pressure of the liquid need to be sufficiently small since otherwise the droplets may evaporate. The vapor pressure of ethylene-glycol is $p_{vap} = 5.3$ Pa at ambient conditions compared to $p_{vap} = 3170$ Pa for water. I.e., the size of the ethylene-glycol droplets is likely to be constant during the operation time of the µPIV set-up. However, another

problem arises for liquid droplets, i.e., the condensation of the droplets inside the feeding channels and on the surface of the test section if the gas flow is saturated with aerosol material and the dew-point is reached. A way to overcome that problem is the heating of the surfaces and the feeding channels. Additionally, droplet agglomeration and clogging can occur if the feeding tubes are improperly designed, e.g., step-like diminution of the feeding channels to adopt for the size of the micro-channels. The feeding tubes should be as short as possible to avoid droplet agglomeration-effects.

Most aerosol generators operate in a pressure regime that results in exit-velocities of the device and volume fluxes that are far from those that are necessary for the operation of a fuel cell like micro-channel configuration (see subsection 3.1). I.e., to seed gas flows in micro-channels only a partial volume flux of the aerosol generator can be used. The volume flux inside the micro-channel can be simply adjusted by a valve at the exit of the micro-channel device.

3. EXPERIMENTAL AND NUMERICAL VALIDATION OF THE PARTICLE DEVIATION

In our investigation the suitability of ethylene-glycol particles to seed micro-channel devices is analyzed. Therefore the gas-flow inside a 90° elbow micro-channel is measured using µPIV. The seeding of the flow with ethylene-glycol particles was achieved using different aerosol generators. A partial flux of the generated aerosol was used and the volume flux inside the micro-channel was controlled by a valve at the exit of the channel. The particle generator nebulizes the liquid due to a low-pressure suction effect since the air jet is oriented perpendicular to the small orifice of the liquid-reservoir. The particle size is controlled by a cyclone flow inside the particle generator, i.e., huge droplets are separated due to inertia and only tiny particles may leave the central exit orifice at the top of the seeder.

Previously to the µPIV measurements the size and the concentration of the particles generated with different particle seeders are measured. A TSI3321 Aerodynamic Particle Sizer (APS) was used. This device measures the size of the particles in a range of 0.5-20µm based on a time-of-flight technique. The particles pass two partially overlapping laser beams such that per particle two intensity peaks can be detected. The time between these intensity peaks is a direct measure of the aerodynamic diameter of the particle. The light-scattering of the particles is used to measure the particle concentration. The particles are generated by three different seeders operated with pressurized air : a) a home-made Laskin-Seeder, b) seeder from LaVision GmbH, c) seeder from Palas GmbH.

For our experiments with ethylene-glycol the most suitable particle size distribution was achieved with the Laskin-Seeder, i.e., highest particle concentration at a particle size of approximately 1 µm and lowest relative amount of larger particles. The particle diameter that corresponds to the distribution maximum is $d_p \approx 1.2$ µm at a concentration of $c_p \approx 6.6 \times 10^3$ cm^{-3} as depicted in Fig. 2. Note, the similar measurements have been performed with DEHS and Novec7500-liquid using the Palas aerosol generator. We found a slightly smaller diameter but lower concentrations for DEHS. Novec7500 can be atomized at high concentrations achieving small diameters but Rh-B cannot be dissolved in this liquid. Hence, ethylene-glycol seems to be
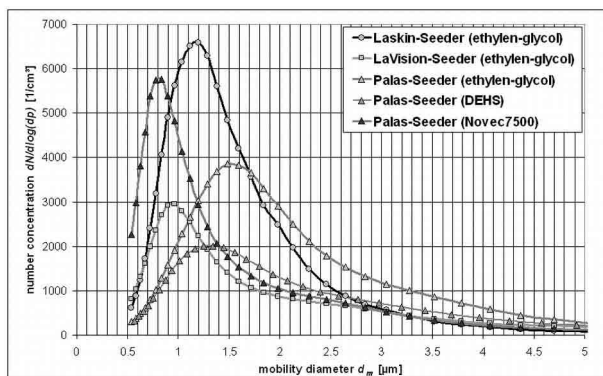
Figure 2 : *Particle-size distribution for different aerosol materials and different aerosol generators*

superior to the other seeding materials. The flow field inside the 90° elbow is investigated for a typical Reynolds number concerning PEM fuel cells, i.e., $Re \approx 200$. This Reynolds number which is based on the micro-channel width corresponds to mean velocities of $u_{mean} = 3.5$ m/s. The flow is in the laminar regime. For fully developed flows in a square channel a hyperbolic velocity profile exists and the maximum velocity is approximately twice the mean velocity [8]. The micro-channel is 1 mm wide and 0.96 mm deep. Hence, assuming a quarter-circle curved path of the streamlines in the 90° elbow the deviation of the particle traces from the streamlines can be assessed using eq. 4. The particle response time for 1.2 μm diameter ethylene-glycol particles in air is $\tau = 5$ μs. Corresponding to eq. 4 the deviation on a quarter-circle path would be $s_{P,\tau} = 114$ μm (11.4 % of the channel width) for $u_{max} = 7$ m/s. Note, due to lateral pressure gradients the velocity profile is distorted in the curved region and hence, the maximum occurring velocity in the curved region can be expected to be smaller. However, the achieved particles sizes are supposed to sufficiently map the flow field in the elbow region of the micro-channel. μPIV measurements and CFD calculations are performed to analyze the ability of these ethylene-glycol particles in detail.

The PIV set-up consists of a Zeiss Axio-Observer Z1 epi-fluorescence microscope with a 12 bit PCO Sensicam QE and a Newave Pegasus frequency-doubled Nd :YLF laser. The Davis 7.2 PIV software from LaVision is used. The seeding density inside the micro-channel is relatively low, since only a part of the volume flux of the seeder is used. The use of a valve to control the volume flux inside the channel leads to small seeding densities at low channel velocities. I.e., the application of standard cross-correlation methods is not suitable. However, since the flow is stationary, averaging techniques can be applied. In our case the sum-of-correlation technique is used [13], [21]. Using adaptive cross-correlation schemes with an interrogation window overlap of 50 % leads to a final vector spacing of 32 x 32 pixels, i.e., a final spatial resolution of 38 μm for the velocity data.

To validate the measurement results in the gas-phase the same Reynolds number cases are investigated using water as working fluid and 8 μm MF particles. Due to the small density difference the deviation of these particles is negligible. Since the MF-particles can be pre-mixed into the water an adequate seeding density can be adjusted and conventional PIV evaluation methods can be applied. Additionally to the experimental investigations, 3D-CFD calculations are performed using FLUENT to quantify the deviation of ethylene-glycol particles of different diameters in air. The results of

the μPIV measurements and the CFD calculations are presented in the following.

As depicted in Fig. 3 very similar flow structures were detected for the gas-flow and the water-flow cases. Obviously, in the case of $Re = 200$ a three-dimensional flow field occurs, since the Dean number [4] is larger than 30. Even in this case, the fluid motion seems to be adequately mapped in the gas-flow using ethylene-glycol particles, since no significant deviation between the depicted velocity vectors in the water-flow and the gas-flow measurements are visible. The PIV measurement in the gas-flow case seems to be based on the particle motion of the smaller particles of the spectrum, i.e., on the particles of $d_p = O(1$ μm$)$, since larger particles would lead to significant deviations of the particle traces from the streamlines. Note, since the sum-of-correlation technique is applied for the PIV evaluation in the gas-flow case the correlation peaks resulting from the motion of large but few particles (compare the spectrum given in Fig. 2) may be significantly reduced such that the resulting highest correlation peak corresponds to the motion of small particles. However, some larger particles are present in the flow and these particles lead to problems : Due to centrifugal forces and the emerging Dean-vortices large particles collide with the channel wall. Fluorescence agglomerates and increases with time. On the one hand, this locally changing brightness affords a severe image pre-processing that also eliminates valid particle signals, on the other hand this huge region of bright fluorescence superimposes by-passing particles such that a PIV evaluation in these regions is hindered

The CFD-results reveal similar flow patterns as in the experimental investigations as depicted in Fig. 4. The flow structure is visualized by particle traces. Light grey particle traces belong to 300 nm particles. The response time and deviation of these particles is sufficiently low, i.e., these particles can be regarded to map the flow almost perfectly. The darker particle traces belong to 1 μm-particles. As can be seen, the traces slightly deviate in the rear part of the elbow section. Note the distance between the indicated exemplary particle traces. This distance is in the order of 30 μm. Again calculating the deviation of a particle on a quarter-circle
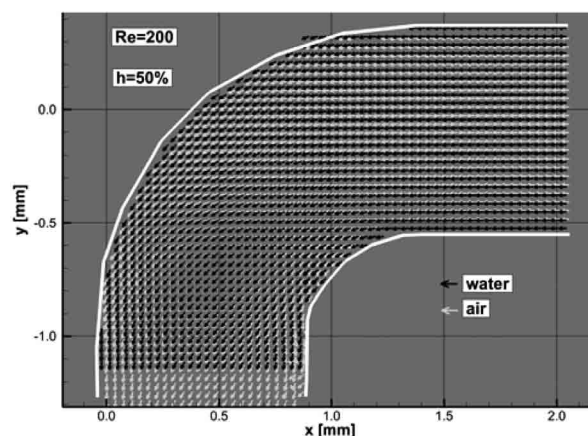

Figure 3 : *Normalized velocity distribution in the 90° elbow channel at Re = 200 for the gas-phase (bright vectors) and the water μPIV-measurements (black vectors).*

4. The Dean number is defined as follows : $De = Re\sqrt{a/(2R)}$ with a being the channel width and R being the curvature radius. At $De < 30$ no secondary flow structure evolves due to centrifugal effects.
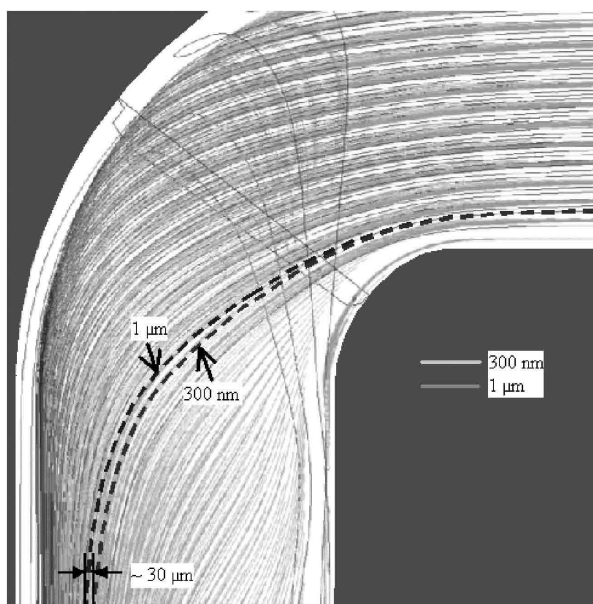
Figure 4 : *CFD calculations of the 3D air flow in a 90° elbow at Re = 200. The traces of 300 nm particles (light grey) and 1 μm particles (grey) are shown.*

curved path as in the previous section leads to a deviation of approximately 52 μm taking into account an initial velocity of 4.5 m/s at the beginning of the curvature of this particle path, i.e., in the elbow entrance region. Note, in this case the fluid motion is more complex than that of a simple quarter-circle path since Dean vortices occur and the velocity profile is deformed due to flow separation. However, in the selected region the inertia-induced particle deviation becomes obvious. In conclusion, the simple calculation of the particle deviation seems to be an effective tool to assess inertia effects on the particle traces with respect to the streamlines of the flow field of a curved channel structure. The calculated values even overestimate the expected deviations.

4. DISCUSSION AND CONCLUSION

The previously depicted results clearly indicate that μPIV applications in gas flows in micro-channels are possible but strongly depend on an accurate preparation of the experiment concerning the particle generation. Although small Reynolds numbers are to be investigated the analysis and the experimental and numerical results evidenced that the particle sizes need to be within a small range in the order of 1 μm to be able to follow the flow sufficiently. The acceptable particle range depends on the particle material, i.e., a liquid of a lower density may allow larger particles. However concerning the application of μPIV the fluorescence of the particle material is a key parameter. A strong fluorescence also allows smaller particles. Several tests revealed that ethylene-glycol is a suitable material for the application of μPIV in gas-flows since this material can be easily nebulized and the size of the resulting particles may be adjusted by changing the viscosity by mixing with water. The fluorescent pigment Rhodamine-B easily dissolves in ethylene-glycol such that strong fluorescence intensities can be detected by the μPIV system. In the present experiment particle sizes between 500 nm and 10 μm could be generated with a distribution maximum at 1.2 μm. The μPIV measurements in a 90° elbow micro channel based on this particle size dis-

tribution proved that the flow structure could be mapped by the particle traces in an acceptable manner. However, the amount of larger particles is supposed to lead to erroneous μPIV results although the sum-of-correlation method seems to minimize this error. Furthermore, large particles impact on the channel walls due to centrifugal forces. Large areas are covered with fluorescent material that hinders the μPIV post-processing. Especially concerning the intended application of this μPIV technique to fuel cells this is not acceptable. Hence, although the particle material itself seems to be suitable to extend the μPIV technique to gas-phase flows and especially to the application in fuel cells the particle generation is a key mechanism that needs to be optimized. The generation of monodispers particles is the next and inevitable step towards μPIV in gas-phase flows.

REFERENCES

[1] Bindhu C. V. & Harilal S. S. (2001) — Effect of the Excitation Source on the Quantum-Yield Measurements of Rhodamine-B Laser Dye Studied Using Thermal-Lens Technique. *Analytical Sciences.* **17** 141-144

[2] Feser J. P. ; Prasad A. K. & Advani S. G. (2007) — Particle Image Velocimetry Measurements in a Model Proton Exchange Membrane Fuel Cell. *J. Fuel Cell Sci. Technol.* **4** 328-335

[3] Grega L. ; Mcgarry M. ; Begum M. & Abruzzo B. (2007) — Flow Characterization of a Polymer Electronic Membrane Fuel Cell Manifold and Individual Cells Using Particle Image Velocimetry. *J. Fuel Cell Sci. Technol.* **4** 272-279

[4] Heinzel A., Mahlendorf F., Roes J. (2006) — *Brennstoffzellen : Entwicklung, Technologie, Anwendung. C.F. Müller Verlag, Heidelberg.*

[5] Hidrovo C. H. ; Kramer T. A. ; Wang E. N. ; Vigneron S. ; Steinbrenner J. E. ; Koo J. ; Wang F. ; Fogg D. W. ; Flynn R. D. ; Lee E. ; Cheng C. ; Kenny T. W. ; Eaton J. K. & Goodson K. E. (2006) — Two-Phase Microfluidics for Semiconductor Circuits and Fuel Cells. *Heat Transfer Engineering.* **27(4)** 53-63

[6] Hinds W. C. (1999) — Aerosol Technology – Properties, Behavior, and Measurement of Airborne Particles. Jon Wiley and Sons, New York

[7] Huang C. ; Shy S. ; Chien C. & Lee C. (2010) — Parametric study of anodic microstructures to cell performance of planar solid oxide fuel cell using measured porous transport properties. *J Power Sources.* **195** 2260–2265

[8] Johnson R. W. (Ed.) (1998) — *The Handbook of Fluid Mechanics, CRC Press LLC.*

[9] Kucernak A., Ladewig B., Blewitt R. & Shrimpton J. (2005) — Laser Doppler Anemometry Study of Reactant Flow in Fuel Cell Channels. *3rd European PEFC Forum, Lucerne.* Poster 21

[10] LEBAEK J. ; ANDREASEN M. B. ; ANDRESEN H. A. ; BANG M. & KAER S. K. (2010) — Particle Image Velocimetry and Computational Fluid Dynamics Analysis of Fuel Cell Manifold. *J. Fuel Cell Sci. Technol.* 031001-1-031001-10

[11] LI H., TANG Y., WANG Z., SHI Z., WU S., SONG D., ZHANGM J., FATIH K., ZHANG J., WANG H., LIU Z., ABOUATALLAH R., MAZZA A. (2008) — A review of water flooding issues in the proton exchange membrane fuel cell. *J Power Sources.* **178** 103-117

[12] LI X. & SABIR I. (2005) — Review of bipolar plates in PEM fuel cells : Flow-field designs. *Int. J. Hydrogen Energy.* **30** 359-371

[13] LINDKEN R., ROSSI M., GROSSE S. & WESTERWEEL J. (2009) — Micro-Particle Image Velocimetry (μPIV) : Recent developments, applications, and guidelines. *Lab Chip.* **9** 2551-2567

[14] LINDKEN R., WESTERWEEL J. & WIENECKE B. (2006) — Stereoscopic Micro Particle Image Velocimetry. *Exp Fluids.* **41** 161-171

[15] MARTIN J. ; OSHKAI P. & DJILALI N. (2005) — Flow Structures in a U-Shaped Fuel Cell Flow Channel : Quantitative Visualization Using PIV. *J. Fuel Cell Sci. Technol.* **2** 70-80

[16] OLSEN M.G. & ADRIAN R.J. (2000) — Out-of-focus effects on particle image visibility and correlation in microscopic Particle Image Velocimetry. *Exp Fluids.* **29(7)** 166-174

[17] RAFFEL M., WILLERT C., & KOMPENHANS J. (2007) — *Particle Image Velocimetry – A Practical Guide. Springer Verlag, Berlin-Heidelberg*

[18] SUGII Y. & OKAMOTO K. (2006) — Velocity Measurement of Gas Flow Using Micro PIV Technique in Polymer Electrolyte Fuel Cell. *Proceedings of ICNMM2006 Fourth International Conference on Nanochannels, Microchannels and Minichannels, June 19-21, 2006, Limerick, Ireland*

[19] VAN DER SCHOOT N. ; BURGMANN S. ; ASBACH C. ; WARTMANN J. ; HEINZEL A. & LINDKEN R. (2010) — Entwicklung der Mikro Particle Image Velocimetry Methode für Gasphasenströmung in Mikrokanälen. *Fachtagung "Lasermethoden in der Strömungsmesstechnik" 7–9 September 2010, Cottbus*

[20] VAN DER SCHOOT N. ; LINDKEN R. ; SHARP K. V. ; PEIL S. ; WARTMANN J. & WESTERWEEL J. (2008) — PIV-Messungen zur Untersuchung in Brennstoffzellen. *Fachtagung "Lasermethoden in der Strömungsmesstechnik" 9–11 September 2008, Karlsruhe*

[21] WERELEY S. T. & MEINHART C. D. (2009) — Recent Advances in Micro-Particle Image Velocimetry. *Annu. Rev. Fluid Mech.* **42** 557-576

[22] WIENECKE B. (2010) — *LaVision GmbH, personal communication*

[23] YAN W., YANG C., SOONG C., CHEN F., MEI S. (2006) — Experimental studies on optimal operating conditions for different flow field designs of PEM fuel cells. *J Power Sources.* **160** 284-292

[24] YARIN A. ; TROPEA C. & FOSS J. F. (EDS.) (2007) — *Handbook of Experimental Fluid Mechanics, Springer*

[25] YOON S. ; ROSS J. ; MENCH M. & SHARP K. (2006) — Gas-phase Particle Image Velocimetry (PIV) for application to the design of fuel cell reactant flow channels. *J Power Sources.* **160** 1017–1025